Inorganica Chimica Acta 362 (2009) 2722–2727

Contents lists available at ScienceDirect

Inorganica Chimica Acta

journal homepage: www.elsevier.com/locate/ica

Synthesis and structures of zinc complexes with new binucleating ligands containing alkoxide bridges, and their activities in the hydrolysis of tris(*p*-nitrophenyl)phosphate

Katsura Mochizuki [a,*], Yukiko Ishima [a], Kiyoharu Hayano [b]

[a] International Graduate School of Arts and Sciences, Yokohama City University, Yokohama 236-0027, Japan
[b] Hokkaido University of Education Sapporo, Sapporo 002-8502, Japan

ARTICLE INFO

Article history:
Received 1 October 2008
Received in revised form 8 December 2008
Accepted 12 December 2008
Available online 25 December 2008

Keywords:
Zinc complexes
Binucleating ligands
Synthesis
Hydrolysis

ABSTRACT

Four new binucleating ligands featuring a hydroxytrimethylene linker between two coordination sites (1,3-bis{*N*-[3-(dimethylamino)propyl]-*N*-methylamino}propan-2-ol, **HL^1**; 1,3-bis{*N*-[2-(dimethylamino)ethyl]-*N*-methylamino}propan-2-ol, **HL^2**; 1,3-bis[bis(2-methoxyethyl)amino]propan-2-ol, **HL^3**; and 1-bis[(2-methoxyethyl)amino]-3-{*N*-[2-(dimethylamino)ethyl]-*N*-methylamino}propan-2-ol, **HL^4**) were synthesized, along with the corresponding zinc complexes. The structures of three dinuclear zinc complexes ($[Zn_2\mathbf{L^1}(\mu\text{-}CH_3COO)_2]BPh_4$ (**1**), $[Zn_2\mathbf{L^3}(\mu\text{-}CH_3COO)_2]BPh_4$ (**3**), and $[Zn_2\mathbf{L^4}(\mu\text{-}CH_3COO)(CH_3COO)(EtOH)]BPh_4$ (**4**)) and a tetranuclear zinc complex ($\{[Zn_2\mathbf{L^2}(\mu\text{-}CH_3COO)]_2(\mu\text{-}OH)_2\}(BPh_4)_2$ (**2**)) were revealed by X-ray crystallography. Hydrolysis of tris(*p*-nitrophenyl)phosphate (TNP) by these zinc complexes in an acetonitrile solution containing 5% Tris buffer (pH 8.0) at 30 °C was investigated spectrophotometrically and by ^{31}P NMR. Although zinc complexes **1**, **3**, and **4** did not show hydrolysis activity, the tetranuclear zinc complex **2**, containing μ-hydroxo bridges, was capable of hydrolyzing TNP. This suggests that the hydroxide moiety in the complex may have an important role in the hydrolysis reaction.
© 2008 Elsevier B.V. All rights reserved.

1. Introduction

It is well known that the active sites of a number of enzymes contain metal ions [1,2]. Dinuclear metal sites in enzymes have been the subject of particular attention from coordination chemists, especially with respect to the relationship between structure and function. Accordingly, many binucleating ligands have been synthesized and used in complexes modeling dinuclear metal sites [1–3]; in particular, extensive studies have been carried out using dinickel(II) complexes to model the active site of urease [4] and dizinc(II) complexes to model the trinuclear sites of P1 nuclease [5] and alkaline phosphatase [5]. One strategy for the synthesis of binucleating ligands involves the use of a 2-hydroxytrimethylene linker which can bridge two metal ions proximately via an alkoxide moiety [6–17]. In previous studies, we synthesized binucleating bis(macrocyclic) ligands and studied their dinuclear metal complexes [18–20]. In the course of our synthesis of a bis(macrocyclic) ligand containing a 2-hydroxytrimethylene bridge, it was incidentally found that methylation of the hexaamine ligand (**HL**) [20] used as a starting material for the bis(macrocycle) resulted in dealkylation of the *N,N*-dimethylaminopropyl arms to afford a potentially binucleating ligand (**HL^1**, Scheme 1) [21]. In this work, in order to investigate the coordination behavior of such ligands, we synthesized four new binucleating ligands (**HL^1**, **HL^2**, **HL^3**, and **HL^4**) containing a 2-hydroxytrimethylene linker between the two coordination sites, as well as the corresponding zinc complexes. The formation of dinuclear (**HL^1**, **HL^3**, and **HL^4**) and tetranuclear (**HL^2**) zinc complexes was confirmed by X-ray crystallography. In addition, the hydrolysis reaction of tris(*p*-nitrophenyl)phosphate (TNP) by these zinc complexes was investigated.

2. Experimental

2.1. Synthesis of binucleating ligands

1,3-Bis{N-[3-(dimethylamino)propyl]-N-methylamino}propan-2-ol (**HL^1**): To an ethanol solution (10 ml) of *N,N,N′*-trimethyl-1,3-propanediamine (2.0 g, 17.21 mmol) were added triethylamine (3.0 g, 29.65 mmol) and epichlorohydrin (0.8 g, 8.65 mmol), and the mixture was refluxed for 15 h. The solution was then evaporated to half its original volume and basified to ca. pH 12 by the addition of a 6 mol dm^{-3} NaOH solution. The product was extracted three times with dichloromethane (10 ml). The yellow extract was dried over sodium sulfate and evaporated to dryness to yield viscous oil. The free ligand was purified by conversion of the crude ligand to its hydrochloride salt and re-extraction of the

* Corresponding author. Tel.: +81 45 787 2186; fax: +81 45 787 2413.
E-mail address: katsura@yokohama-cu.ac.jp (K. Mochizuki).

0020-1693/$ - see front matter © 2008 Elsevier B.V. All rights reserved.
doi:10.1016/j.ica.2008.12.012

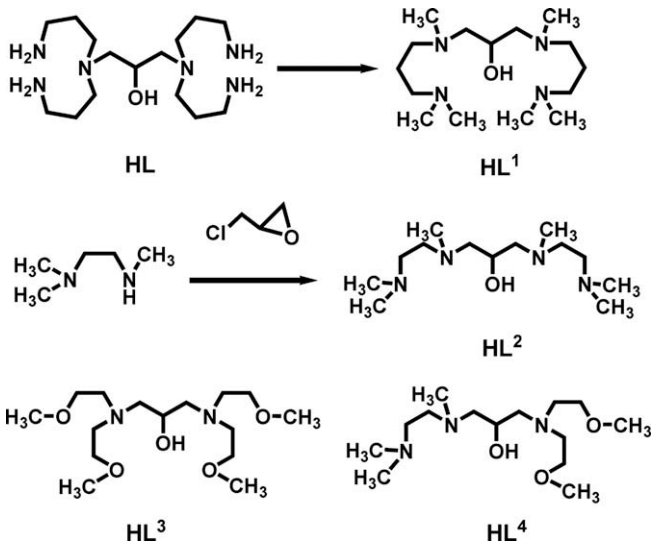

Scheme 1. Syntheses and structure formulae.

ligand from a basic aqueous solution. Yield: 83%. HRMS (APCI) calc. for $[C_{15}H_{36}N_4O_1+H]^+$: *m/z* 289.2967, found: *m/z* 289.2967. ^{13}C NMR ($CDCl_3$): δ 25.6 (t), 43.0 (q), 45.6 (q), 55.9 (t), 57.9 (t), 62.3 (t), 66.0 (d) ppm.

1,3-Bis{N-[2-(dimethylamino)ethyl]-N-methylamino}propan-2-ol (**HL²**): **HL²** was prepared by a similar procedure to **HL¹**, but using *N,N,N′*-trimethylethylenediamine instead of *N,N,N′*-trimethyl-1,3-propanediamine. Yield: 41%. HRMS (EI) calc. for $[C_{13}H_{33}N_4O_1]^+$: *m/z* 261.2654, found: *m/z* 261.2646. ^{13}C NMR ($CDCl_3$): δ 43.4 (q), 45.3 (q), 55.7 (t), 57.1 (t), 62.0 (t), 66.1 (d) ppm.

1,3-Bis[bis(2-methoxyethyl)amino]propan-2-ol (**HL³**): **HL³** was prepared by a similar method to **HL¹** and using bis(2-methoxyethyl)amine. Yield: 59%. HRMS (APCI) calc. for $[C_{15}H_{34}N_2O_5+H]^+$: *m/z* 323.2546, found: *m/z* 323.2561. ^{13}C NMR ($CDCl_3$): δ 54.5 (q), 58.2 (t), 59.2 (t), 66.5 (d), 71.0 (t) ppm.

1-Bis[(2-methoxyethyl)amino]-3-{N-[2-(dimethylamino)ethyl]-N-methylamino}propan-2-ol (**HL⁴**): To an ethanol solution (10 ml) of epichlorohydrin (1.4 g, 15.13 mmol) was added dropwise an ethanol solution (5 ml) of bis(methoxyethyl)amine (2.0 g, 15.02 mmol). After the mixture had been heated at 80 °C for 3 h, the solution was cooled to 60 °C and NaOH (0.60 g, 15.0 mmol) in a minimum amount of water was added. *N,N,N′*-Trimethylethylenediamine (1.50 g, 14.7 mmol) was added to the mixture, which was then further heated at 80 °C for 3 h. The solution was cooled to room temperature, evaporated to its half volume, and basified to ca. pH 12 by the addition of a 6 mol dm^{-3} NaOH solution. The product was extracted with dichloromethane (10 ml) three times. The resulting yellow extract was dried over sodium sulfate and evaporated to dryness to yield a yellow viscous oil (3.2 g). The crude free ligand was purified by column chromatography on silica gel (Merck silica gel 60, $CHCl_3$:MeOH = 1:1). Yield: 1.43 g, 33%. HRMS (EI) calc. for $[C_{14}H_{34}N_3O_3]^+$: *m/z* 292.2600, found: *m/z* 292.2602. ^{13}C NMR ($CDCl_3$): δ 43.2 (q), 45.0 (q), 54.7 (t), 55.0 (t), 56.8 (t), 58.5 (q), 59.4 (t), 61.7 (t), 66.3 (d), 70.9 (t) ppm.

2.2. Synthesis of zinc complexes

$[Zn_2L^1(\mu\text{-}CH_3COO)_2]BPh_4$ (**1**): To an ethanol solution (5 ml) of **HL¹** (0.20 g, 0.70 mmol) was added $Zn(CH_3COO)_2{\cdot}2H_2O$ (0.33 g, 1.50 mmol), and the solution was heated at 60 °C for 2 h. The addition of $NaBPh_4$ (0.24 g, 0.70 mmol) resulted in the formation of a white precipitate, which was filtered and dried in vacuum. Yield: 0.29 g, 56%. HRMS (FAB) calc. for $[C_{19}H_{41}N_4O_5{}^{64}Zn_2]^+$: *m/z* 533.1660, found: *m/z* 533.1662. IR (KBr): ν 1601 cm^{-1} (CH_3COO^-), 1470 cm^{-1}, 1429 cm^{-1}, 704 cm^{-1}. Crystals suitable for X-ray analysis were obtained by recrystallization from acetonitrile/ethanol.

$\{[Zn_2L^2(\mu\text{-}CH_3COO)]_2(\mu\text{-}OH)_2\}(BPh_4)_2$ (**2**): To an ethanol solution (5 ml) of **HL²** (0.130 g, 0.50 mmol) was added $Zn(CH_3COO)_2{\cdot}2H_2O$ (0.24 g, 1.09 mmol), and the solution was heated at 60 °C for 2 hours. The addition of $NaBPh_4$ (0.40 g, 1.17 mmol) resulted in the formation of a white precipitate, which was filtered and dried in vacuum. Yield: 0.16 g, 41%. *Anal.* Calc. for $C_{78}H_{110}N_8O_8B_2Zn_4$: C, 59.64; H, 7.06; N, 7.13. Found: C 59.48, H 7.27, N 7.05%. MS (ESI): *m/z* 1251.4 $[M\text{-}BPh_4]^+$, 465.1 $[Zn_2L^2(CH_3COO)(OH)]^+$. IR (KBr): ν 3656 cm^{-1} sharp (OH^-), 1593 cm^{-1} (CH_3COO^-), 1466 cm^{-1}, 1421 cm^{-1}, 706 cm^{-1}. Crystals suitable for X-ray analysis were obtained by recrystallization from nitromethane/diethylether.

$[Zn_2L^3(\mu\text{-}CH_3COO)_2]BPh_4$ (**3**): To an ethanol solution (5 ml) of **HL³** (0.10 g, 0.31 mmol) was added $Zn(CH_3COO)_2{\cdot}2H_2O$ (0.14 g, 0.64 mmol). The solution was heated at 60 °C for 2 h. The addition of the $NaBPh_4$ (0.11 g, 0.32 mmol) resulted in the formation of a white precipitate, which was filtered and dried in vacuum. Yield: 0.18 g, 64%. Crystals suitable for X-ray analysis were obtained by recrystallization from nitromethane/diethylether. *Anal.* Calc. for $C_{43}H_{59}N_2O_9B_1Zn_2$: C, 58.06; H, 6.69; N, 3.15. Found: C, 58.28; H, 6.70; N, 3.28%.

$[Zn_2L^4(\mu\text{-}CH_3COO)(CH_3COO)(EtOH)]BPh_4$ (**4**): To an ethanol solution (5 ml) of **HL⁴** (0.10 g, 0.34 mmol) was added $Zn(CH_3COO)_2{\cdot}2H_2O$ (0.20 g, 0.91 mmol), and the solution was heated at 60 °C for 2 h. The addition of $NaBPh_4$ (0.23 g, 0.67 mmol) resulted in the formation of a white precipitate, which was filtered and dried in vacuum. Yield: 0.26 g. *Anal.* Calc. for $C_{44}H_{64}N_3O_8B_1Zn_2$: C, 58.42; H, 7.13; N, 4.63. Found: C, 58.35; H, 7.12; N, 4.73%. Crystals were obtained by recrystallization from nitromethane/diethylether.

2.3. Physical measurements

^{13}C NMR spectra were recorded using a Bruker DRX 300 spectrometer and a JEOL EPC-400 spectrometer. Mass spectra were measured using a JEOL DX-303 spectrophotometer and high resolution mass spectra were measured at the Center for Instrumental Analysis of Hokkaido University.

2.4. Crystallographic studies

X-ray crystallography of single crystals was carried out on a MAC Science MXC3k four-circle (ω-2θ scan: **1** and **3**, **ω-**scan: **2** and **4**) diffractometer with graphite-monochromatized Mo Kα radiation (λ = 0.71073 Å). The structures were solved by the direct method (SIR92 and SIR97 [22]), and refined on F^2 by the full-matrix least-squares method SHELXL-97 [23]). The φ-scan was applied for absorption correction [24]. All non-hydrogen atoms were refined using anisotropic thermal parameters (riding model refinement). Hydrogen atoms were placed by SHELXL [23]. All calculations were carried out using a SiliconGraphics O_2 work station (MAXUS program system provided by MAC Science). Structural diagrams were drawn using ORTEP-3 for Windows [25]. Crystallographic data for the complexes are listed in Table 1. Because $[Zn_2L^4(\mu\text{-}CH_3COO)(CH_3COO)(EtOH)]BPh_4$ (**4**) was unstable in air due to loss of solvent molecules, a crystal covered with epoxy resin was used for measurement. During analysis of **4**, disorder was found in the coordinated ethanol, which was treated using the SHELXL commands PART 1 (65.4%) and PART 2 (34.6%), with restraints on the HO–CH_2 and CH_2–CH_3 distances between the two parts (data/restraints/parameters: 10724/2/545). No restraints were applied for the other complexes.

Table 1
Crystallographic data of complexes.

Complex	**1**	**2**	**3**	**4**
Empirical formula	$BC_{43}H_{61}N_4O_5Zn_2$	$B_2C_{78}H_{110}N_8O_8Zn_4$	$B_1C_{43}H_{59}N_2O_9Zn_2$	$B_1C_{44}H_{64}N_3O_8Zn_2$
Formula weight	855.56	1570.94	889.53	904.59
T (K)	298(2)	298(2)	298(2)	298(2)
λ (Å)	0.71070	0.71070	0.71070	0.71070
Crystal system	triclinic	monoclinic	triclinic	monoclinic
Space group	$P\bar{1}$	$P2_1/c$	$P\bar{1}$	$P2_1/c$
Unit cell dimensions				
a (Å)	9.5640(14)	12.255(4)	10.947(3)	14.247(4)
b (Å)	15.309(2)	13.835(4)	14.260(6)	18.104(3)
c (Å)	16.507(2)	29.425(8)	14.690(3)	18.335(3)
α (°)	74.502(8)		103.26(2)	
β (°)	77.309(10)	120.02(4)	93.34(2)	99.15(2)
γ (°)	83.877(10)		91.14(3)	
V (Å^3)	2269.1(5)	4320(2)	2226.9(11)	4669(2)
Z	2	4	2	4
D_{calc} (Mg m^{-3})	1.252	1.208	1.326	1.287
μ (mm^{-1})	1.102	1.150	1.131	1.079
$F(000)$	904	1656	936	1912
Crystal size (mm)	0.50 × 0.40 × 0.20	0.50 × 0.50 × 0.30	0.50 × 0.20 × 0.20	0.80 × 0.30 × 0.10
Reflections collected	11046	9884	10649	11059
Independent reflections [R_{int}]	10238 [0.0093]	9884 [0.0012]	10236 [0.0447]	10724 [0.0467]
Goodness-of-fit (GOF)	1.153	1.131	1.055	1.019
Final R indices [$I > 2\sigma(I)$]	R_1 = 0.0465, wR_2 = 0.1529	R_1 = 0.0883, wR_2 = 0.2709	R_1 = 0.0674, wR_2 = 0.1957	R_1 = 0.0603, wR_2 = 0.1110
Largest difference in peak and hole (e Å^{-3})	1.923 and −0.705	2.003 and −0.608	1.142 and −0.423	0.529 and −0.450

2.5. Hydrolysis of tris(p-nitrophenyl)phosphate (TNP)

The hydrolysis reactions of tris(*p*-nitrophenyl)phosphate (TNP) by the zinc complexes synthesized in this study were evaluated spectrophotometrically. The zinc complex and TNP were dissolved in an acetonitrile solution containing 5% Tris buffer (2×10^{-3} mol dm^{-3}, pH 8.0) aqueous solution. The spectral change of the mixture from 350 to 500 nm was monitored at 30 °C.

The hydrolysis of TNP in CD_3CN was confirmed by measurement of ^{31}P NMR spectra using a 10 mm tube with 85% phosphoric acid as an external standard in the inner capillary tube. ^{31}P NMR spectra were measured at 26 °C using a JEOL FX-90Q spectrometer.

3. Results and discussion

As dealkylation of the *N,N*-dimethylaminopropyl arms of **HL** to give **HL^1** occurred during a separate investigation [21], in this study we attempted to synthesize **HL^1**, which was expected to act as a binucleating ligand, by another pathway (Scheme 1). **HL^1** was synthesized by the reaction of epichlorohydrin with *N,N′,N′*-trimethylpropanediamine, as were the analogous ligands **HL^2** (*N,N*-dimethylaminoethyl arms), **HL^3** (methoxyethyl arms), and **HL^4** (unsymmetrical arms).

As expected, all ligands synthesized in this study acted as binucleating ligands to form zinc complexes with a ligand-to-metal ratio of 1:2. The hydroxy group in each ligand was deprotonated and coordinated to two zinc ions. Although three of the ligands—**HL^1**, **HL^3**, and **HL^4**—formed dinuclear zinc complexes under similar synthetic conditions, only **HL^2**, which contains *N,N*-dimethylaminoethyl arms, formed a tetranuclear zinc complex, in which two dinuclear units were linked by two hydroxide ions.

In complex **1** (Fig. 1), which contains *N,N*-dimethylaminopropyl arms, the two zinc ions were linked by two acetates and one alkoxide. Zn(1) and Zn(2) adopted five-coordinate geometries consisting of distorted square-pyramids with O(42) and O(43), respectively, at the top. The τ values were 26.5 (Zn(1)) and 37.4 (Zn(2)), where $\tau = (\alpha - \beta)/60 \times 100$ (α and β are the largest and second largest angle of X–Zn–X, respectively: ideal square-pyramid: $\tau = 0$, ideal trigonal bipyramid: $\tau = 100$) [26]. The six-membered rings consisting of Zn(1), N(1), C(2), C(3), C(4), and N(5), and Zn(2), N(9), C(10), C(11), C(12), and N(13) adopted chair conformations. The two methyl groups, C(16) and C(17), were placed in *syn*-geometry with respect to the plane containing N(5), O(20), and N(9), as were the two *N,N*-dimethylaminopropyl arms.

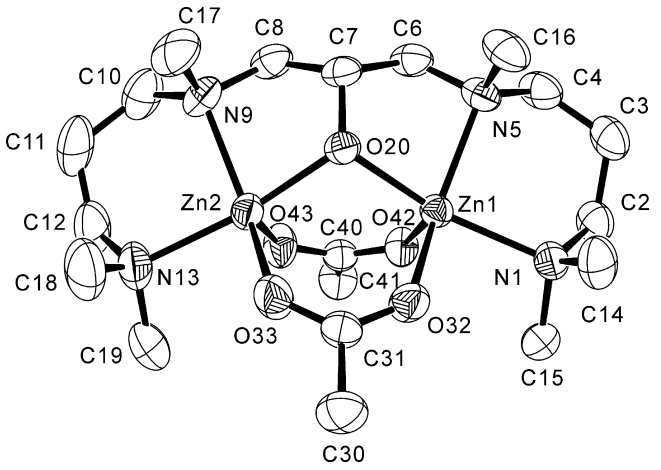

Fig. 1. ORTEP drawing of cation portion of **1**. Selected bond lengths (Å) and angles (°): Zn(1)–O(20) 2.001(2), Zn(1)–O(42) 2.019(2), Zn(1)–O(32) 2.041(2), Zn(1)–N(1) 2.158(3), Zn(1)–N(5) 2.180(3), Zn(2)–O(20) 2.004(2), Zn(2)–O(43) 2.016(3), Zn(2)–O(33) 2.016(3), Zn(2)–N(13) 2.150(3), Zn(2)–N(9) 2.164(3), Zn(1)–Zn(2) 3.2590(6), Zn(1)–O(20)–Zn(2) 108.92(10), O(20)–Zn(1)–O(42) 100.65(9), O(20)–Zn(1)–O(32) 91.63(9), O(42)–Zn(1)–O(32) 105.02(11), O(20)–Zn(1)–N(1) 162.94(10), O(42)–Zn(1)–N(1) 96.12(10), O(32)–Zn(1)–N(1) 86.98(10), O(20)–Zn(1)–N(5) 80.00(10), O(42)–Zn(1)–N(5) 107.82(11), O(32)–Zn(1)–N(5) 147.06(11), N(1)–Zn(1)–N(5) 91.98(11), O(20)–Zn(2)–O(43) 99.26(10), O(20)–Zn(2)–O(33) 91.11(10), O(43)–Zn(2)–O(33) 110.16(13), O(20)–Zn(2)–N(13) 167.03(12), O(43)–Zn(2)–N(13) 93.43(13), O(33)–Zn(2)–N(13) 86.97(12), O(20)–Zn(2)–N(9) 80.45(11), O(43)–Zn(2)–N(9) 105.14(12), O(33)–Zn(2)–N(9) 144.60(13), N(13)–Zn(2)–N(9) 93.73(13).

Complex **1** showed a temperature-dependent ^{13}C NMR spectrum in CD_3CN (Supplementary Fig. S1). At 27 °C, two broad methyl signals were observed around 47 ppm, which were assigned as *N,N*-dimethylamino groups, while at a low temperature (−40 °C) these signals sharpened and appeared clearly at 44.0 and 48.9 ppm. As the temperature was increased, the two methyl signals gradually collapsed, almost disappearing by 60 °C. This

temperature-dependent signal change was reversible and was not observed for the other zinc complexes investigated in this study.

Shortening the arms by replacing trimethylene with ethylene resulted in a dramatic change in coordination geometry. **HL[2]**, containing *N,N*-dimethylaminoethyl arms, formed the tetranuclear zinc complex **2** (Fig. 2), in which two dinuclear units were linked by two hydroxide ions; in the IR spectrum of **2**, a sharp peak was observed at 3656 cm^{-1}, ascribable to ν(OH). An inversion center was present in the middle of the tetranuclear complex. In the dinuclear unit, Zn(1) and Zn(2) adopted five-coordinate distorted trigonal bipyramidal geometries [τ = 74.7 (Zn(1)), τ = 62.2 (Zn(2))] which were different from those of complex **1**; N(4) and O(32), and N(8) and O(33), respectively, were at the top. The five-membered rings consisting of Zn(1), N(1), C(2), C(3), and N(4), and Zn(2), N(8), C(9), C(10), and N(11) adopted *gauche* conformations. The two *N,N*-dimethylaminoethyl arms showed *syn*-geometry with respect to the plane containing N(4), O(20), and N(8). The intra-dinuclear and inter-dinuclear distances between zinc ions were 3.521(1) Å for Zn(1)···Zn(2) and 3.391(1) Å for Zn(1)···Zn(2′), respectively; thus, the Zn···Zn distance when the zinc atoms were linked by a μ-hydroxo bridge was shorter than that of the μ-alkoxo bridge.

HL[3], which contains double methoxyethylene arms, also formed a dinuclear zinc complex **3** (Fig. 3). In the complex, two zinc ions were linked by one alkoxide and two acetates, adopting distorted octahedral six-coordination geometries, in contrast to the complexes described above which contain single-arm ligands. Four five-membered chelate rings around Zn(1) and Zn(2) took *gauche* forms. Two methoxyethyl chains containing O(6) and O(20), respectively, adopted *syn*-geometry with respect to the plane consisting of N(9), O(22), and N(13).

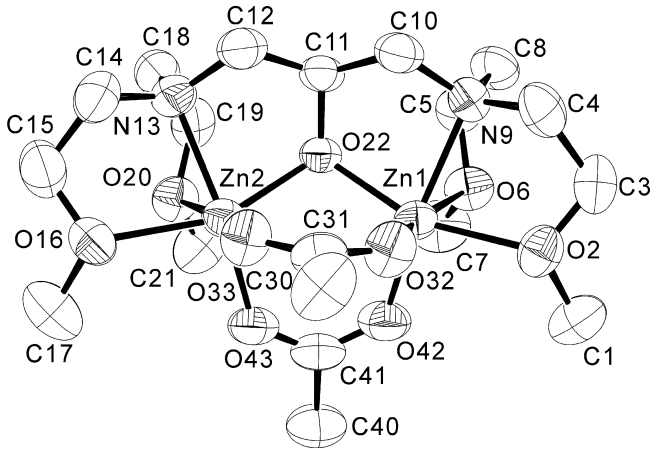

Fig. 3. ORTEP drawing of cation portion of **3**. Selected bond lengths (Å) and angles (°): Zn(1)–O(22) 1.977(4), Zn(1)–O(42) 1.983(5), Zn(1)–O(32) 2.041(4), Zn(1)–O(2) 2.138(5), Zn(1)–N(9) 2.179(5), Zn(1)–O(6) 2.402(5), Zn(2)–O(22) 1.994(4), Zn(2)–O(43) 1.999(5), Zn(2)–O(33) 2.048(5), Zn(2)–N(13) 2.175(5), Zn(2)–O(16) 2.210(5), Zn(2)–O(20) 2.369(5), O(22)–Zn(1)–O(42) 100.3(2), O(22)–Zn(1)–O(32) 98.5(2), O(42)–Zn(1)–O(32) 99.4(2), O(22)–Zn(1)–O(2) 159.8(2), O(42)–Zn(1)–O(2) 98.8(2), O(32)–Zn(1)–O(2) 84.5(2), O(22)–Zn(1)–N(9) 80.8(2), O(42)–Zn(1)–N(9) 160.2(2), O(32)–Zn(1)–N(9) 100.0(2), O(2)–Zn(1)–N(9) 79.0(2), O(22)–Zn(1)–O(6) 90.9(2), O(42)–Zn(1)–O(6) 86.0(2), O(32)–Zn(1)–O(6) 168.0(2), O(2)–Zn(1)–O(6) 84.1(2), N(9)–Zn(1)–O(6) 74.2(2), O(22)–Zn(2)–O(43) 102.0(2), O(22)–Zn(2)–O(33) 99.2(2), O(43)–Zn(2)–O(33) 98.2(2), O(22)–Zn(2)–N(13) 79.9(2), O(43)–Zn(2)–N(13) 161.3(2), O(33)–Zn(2)–N(13) 99.8(2), O(22)–Zn(2)–O(16) 157.5(2), O(43)–Zn(2)–O(16) 99.1(2), O(33)–Zn(2)–O(16) 85.4(2), N(13)–Zn(2)–O(16) 77.6(2), O(22)–Zn(2)–O(20) 90.7(2), O(43)–Zn(2)–O(20) 85.4(2), O(33)–Zn(2)–O(20) 168.4(2), N(13)–Zn(2)–O(20) 76.0(2), O(16)–Zn(2)–O(20) 83.2(2), Zn(1)–O(22)–Zn(2) 106.3(2).

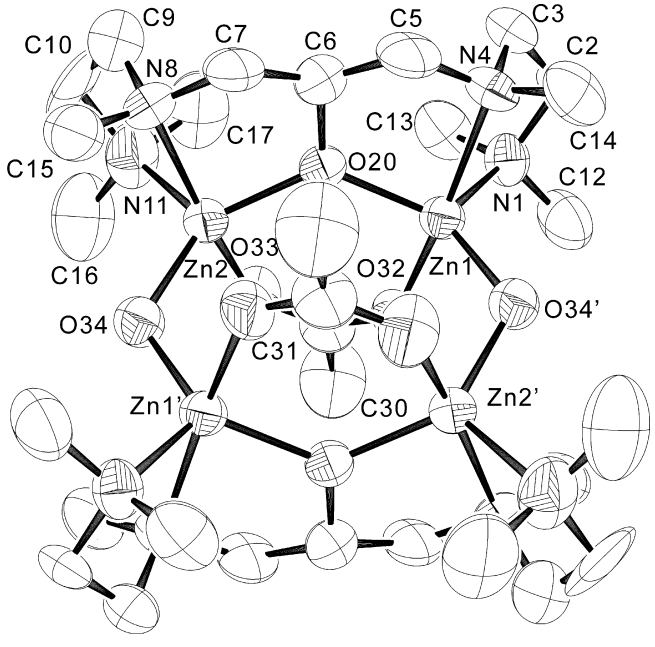

Fig. 2. ORTEP drawing of cation portion of **2**. Selected bond lengths (Å) and angles (°): Zn(1)–O(34′) 1.943(5), Zn(1)–O(20) 1.967(5), Zn(1)–O(32) 2.065(5), Zn(1)–N(1) 2.110(6), Zn(1)–N(4) 2.258(6), Zn(1)–Zn(2) 3.5206(14), Zn(2)–O(20) 1.953(5), Zn(2)–O(34) 1.964(5), Zn(2)–O(33) 2.083(6), Zn(2)–N(11) 2.150(7), Zn(2)–N(8) 2.223(7), O(34′)–Zn(1)–O(20) 126.5(2), O(34′)–Zn(1)–O(32) 92.4(2), O(20)–Zn(1)–O(32) 95.8(2), O(34′)–Zn(1)–N(1) 16.3(2), O(20)–Zn(1)–N(1) 116.2(2), O(32)–Zn(1)–N(1) 91.4(2), O(34′)–Zn(1)–N(4) 95.6(2), O(20)–Zn(1)–N(4) 82.0(2), O(32)–Zn(1)–N(4) 171.3(2), N(1)–Zn(1)–N(4) 82.1(2), O(20)–Zn(2)–O(34) 129.1(2), O(20)–Zn(2)–O(33) 95.7(2), O(34)–Zn(2)–O(33) 94.0(3), O(20)–Zn(2)–N(11) 116.9(3), O(34)–Zn(2)–N(11) 113.5(3), O(33)–Zn(2)–N(11) 86.6(3), O(20)–Zn(2)–N(8) 83.1(2), O(34)–Zn(2)–N(8) 97.3(3), O(33)–Zn(2)–N(8) 166.4(3), N(11)–Zn(2)–N(8) 82.0(3), Zn(2)–O(20)–Zn(1) 127.8(2), Zn(1′)–O(34)–Zn(2) 120.4(3).

It can be seen that the presence of *N,N*-dimethylaminoethyl and *N,N*-dimethylaminopropyl arms favored five-coordination geometry for zinc, while double methoxyethyl arms favored six-coordination. The non-symmetrical ligand **HL[4]**, bearing *N,N*-dimethylaminoethyl and double methoxyethyl arms, formed the dinuclear zinc complex **4** (Fig. 4), which featured two kinds of coordination geometry—a distorted square-pyramidal five-coordinate structure (τ = 39.6, with N(20) at the top) for Zn(1) and the *N,N*-dimethylaminoethyl arm, and a distorted octahedral six-coordinate structure for Zn(2) and the bis(methoxyethylene) arm. The most remarkable feature of this complex, which was not seen in the symmetrical zinc complexes, is that the acetate oxygen atom O(25), coordinated to Zn(1) as a monodentate ligand, is thought to interact through hydrogen bonding (ca. 2.68 Å) with the ethanol oxygen atom O(21) which is coordinated to Zn(2).

The relationship between the Zn···Zn distance and the Zn–O(alkoxo)–Zn angle of the μ-acetato bridge may be discussed with reference to the various zinc complexes. The Zn···Zn distances in the complexes with double μ-acetato bridges, (**3**: 3.179(2) Å, **1**: 3.2590(6) Å), were shorter than those in the complexes with single μ-acetato bridges (**4**: 3.4360(8) Å, **2**: 3.521(1) Å). Moreover, the Zn···Zn distance was reasonably proportional to the Zn–O(alkoxo)–Zn angle (**3**: 106.3(2)°, **1**: 108.92(10)°, **4**: 121.85(13)°, and **2**: 127.8(2)°). Thus, it was concluded that the Zn···Zn distance in these dinuclear complexes is strongly influenced by the number of μ-acetato bridges.

Tetranuclear zinc complexes with analogous structures have been reported previously, including a μ-phenoxo and μ-hydroxo bridged complex [27], a μ-alkoxo and μ-acetato bridged complex [28], and a μ-phenoxo and μ-hydroxo bridged complex **5** [29]. In **5**, two dinuclear zinc complexes with phenoxo linkages are further bridged by two hydroxides, similarly to the tetranuclear complex synthesized in this study. The Zn···Zn distance in the dinuclear unit in **2** is 3.521(1) Å, which is longer than that of the phenoxo-

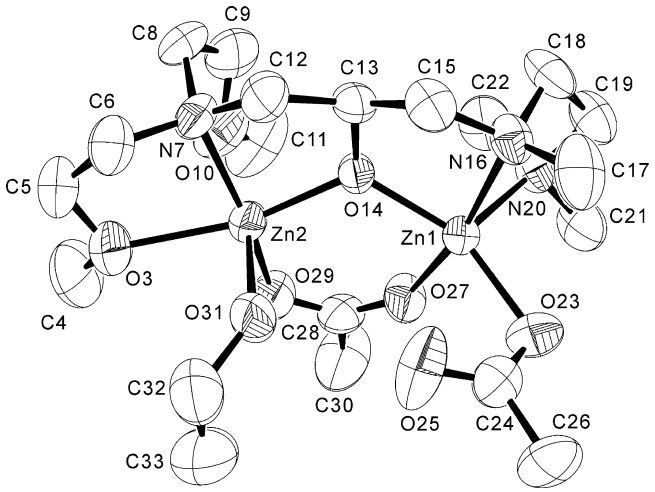

Fig. 4. ORTEP drawing of cation potion of **4** (PART 1). Selected bond lengths (Å) and angles (°): Zn(1)–O(14) 1.958(3), Zn(1)–O(23) 2.006(3), Zn(1)–N(20) 2.097(3), Zn(1)–O(27) 2.118(3), Zn(1)–N(16) 2.239(3), Zn(1)–Zn(2) 3.4360(8), Zn(2)–O(29) 1.950(3), Zn(2)–O(14) 1.973(3), Zn(2)–N(7) 2.130(4), Zn(2)–O(31) 2.151(4), Zn(2)–O(3) 2.238(3), Zn(2)–O(10) 2.272(4), O(14)–Zn(1)–O(23) 145.20(14), O(14)–Zn(1)–N(20) 111.03(13), O(23)–Zn(1)–N(20) 103.15(15), O(14)–Zn(1)–O(27) 90.79(12), O(23)–Zn(1)–O(27) 93.78(14), N(20)–Zn(1)–O(27) 93.12(14), O(14)–Zn(1)–N(16) 80.39(12), O(23)–Zn(1)–N(16) 97.25(14), N(20)–Zn(1)–N(16) 83.99(14), O(27)–Zn(1)–N(16) 168.97(14), O(29)–Zn(2)–O(14) 106.27(13), O(29)–Zn(2)–N(7) 163.36(16), O(14)–Zn(2)–N(7) 82.59(13), O(29)–Zn(2)–O(31) 95.49(18), O(14)–Zn(2)–O(31) 90.44(13), N(7)–Zn(2)–O(31) 98.55(17), O(29)–Zn(2)–O(3) 94.92(15), O(14)–Zn(2)–O(3) 158.68(13), N(7)–Zn(2)–O(3) 77.47(15), O(31)–Zn(2)–O(3) 85.20(14), O(29)–Zn(2)–O(10) 87.36(16), O(14)–Zn(2)–O(10) 97.42(14), N(7)–Zn(2)–O(10) 77.39(15), O(31)–Zn(2)–O(10) 170.55(14), O(3)–Zn(2)–O(10) 85.58(15), Zn(1)–O(14)–Zn(2) 121.85(13).

bridged complex **5** (3.23 Å), although the distances between the dinuclear units are very similar in the two complexes (**2**: 3.39 Å, **5**: 3.41 Å) and are close to that found in the dinuclear zinc active site of P1-nuclease (3.3 Å) [29].

The hydrolysis of tris(*p*-nitrophenyl)phosphate (TNP) by zinc complexes has been reported previously [30–36]. We investigated the abilities of the dinuclear zinc complexes for TNP hydrolysis by spectrophotometric means. Only **2**, a tetranuclear zinc complex with μ-hydroxo bridges, showed activity in this regard. HPLC analysis showed that the hydrolysis product was bis(*p*-nitrophenyl)phosphate (BNP). As shown in Fig. 5, a new absorption band around 380 nm due to the hydrolysis product increased as the reaction proceeded (see Scheme 2). Because this band corresponded to one observed in the reaction between **2** and *p*-nitrophenolate under the same reaction conditions, it was assumed to be due to the formation of a complex between **2** and *p*-nitrophenolate formed during the hydrolysis of TNP. The initial rate of the change in absorption accelerated as the concentration of the zinc complex increased (Supplementary Fig. S2). In addition, the change in absorption was slowed when the pH of the reaction solution was changed from 8.0 to 7.0 and when the water content in the system was lowered from 5% to 1% (see Supplementary Fig. S3). These results suggest that a hydroxo–zinc species (Zn–OH), such as a dinuclear zinc complex with a hydroxide ion, which may be produced by dissociation of the tetranuclear complex, may act as the active species in this hydrolysis reaction. The ^{13}C NMR spectrum of **2** in CD_3CN actually showed more complicated signals than expected for a symmetrical tetranuclear complex, suggesting that the tetranuclear complex may undergo partial dissociation in solution (Supplementary Fig. S4). In addition, the ESI-mass spectrum of **2** in acetonitrile showed the peak at *m/z* 465.1 ascribable

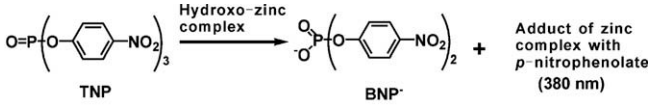

Scheme 2. Hydrolysis of TNP.

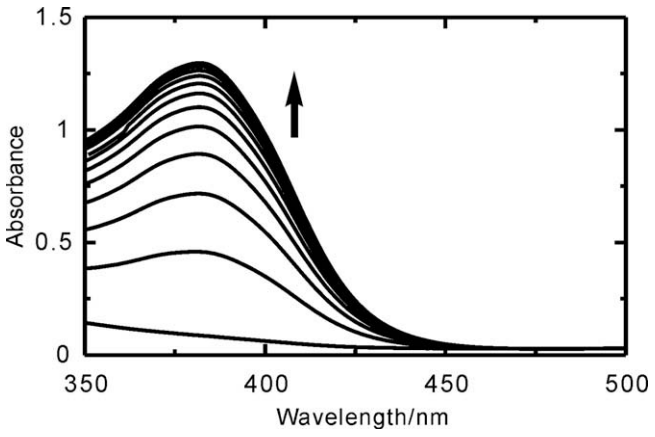

Fig. 5. Change in absorption spectrum during hydrolysis of TNP (1.0×10^{-4} mol dm^{-3}) by complex **2** (5.27×10^{-3} mol dm^{-3}) in an acetonitrile solution containing 5% Tris buffer (pH 8.0) at 30 °C. Scan interval: 10 min.

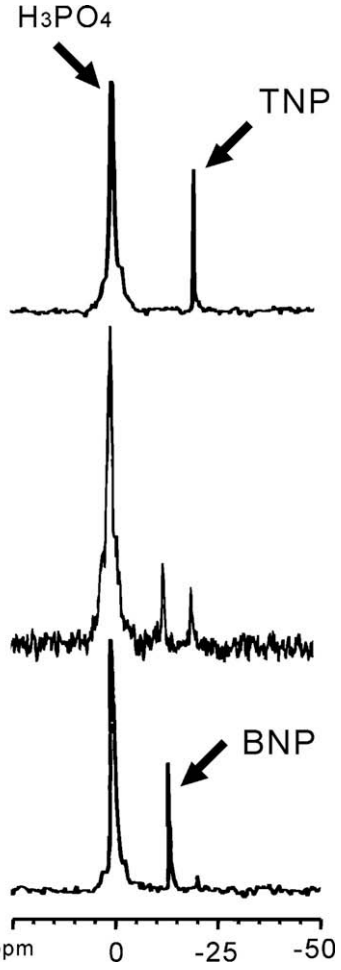

Fig. 6. Change in ^{31}P NMR spectrum during the reaction between TNP (9.78×10^{-3} mol dm^{-3}) and **2** (4.92×10^{-3} mol dm^{-3}) in CD_3CN at 27 °C (upper: before reaction, middle: after 2 days, bottom: after 10 days).

to $[Zn_2\mathbf{L^2}(CH_3COO)(OH)]^+$, which was assumed to arise from the dissociation of **2**.

The hydrolysis of TNP in CD_3CN was confirmed by measurement of ^{31}P NMR spectra. Fig. 6 shows the time dependence of the ^{31}P NMR spectrum measured at 26 °C for a CD_3CN solution containing **2** (4.92×10^{-3} mol dm^{-3}) and TNP (9.78×10^{-3} mol dm^{-3}). The phosphorous signal of TNP appeared at −21 ppm against the reference signal of 85% phosphoric acid at 0.0 ppm. At first, only the signal of TNP was observed. As the reaction proceeded, the signal intensity of TNP decreased but the intensity of the signal ascribed to the hydrolysis product, BNP, at −13.5 ppm increased. After 10 days, the BNP signal was observed with strong intensity, while the TNP signal had become very small. When a ca. tenfold excess of TNP (10.07 mmol dm^{-3}) was reacted with **2** (1.02 mmol dm^{-3}), the integrated TNP:BNP intensity ratio was 4.16:1.0. These results suggest that the tetranuclear zinc complex has the potential to hydrolyze two molecules of TNP in neat CD_3CN. The other zinc complexes, **1**, **3**, and **4**, did not show such hydrolysis activity. It was concluded that the hydroxide bridging dinuclear zinc units is essential for the hydrolysis of the phosphoester bonds of TNP.

In conclusion, new binucleating ligands with various arm structures were synthesized, along with the corresponding zinc complexes, and their structures were determined by X-ray crystallography. Ligand $\mathbf{HL^2}$, which contains *N,N*-dimethylaminoethyl arms, was found to form a tetranuclear zinc complex in which two dinuclear complex units were linked by two hydroxide ions. The tetranuclear zinc complex showed activity for hydrolysis of TNP in aqueous acetonitrile and neat CD_3CN, which was confirmed by visible absorption spectroscopy and ^{31}P NMR studies.

Appendix A. Supplementary material

CCDC 703817, 703818, 703819 and 703820 contain supplementary crystallographic data for **1**, **2**, **3** and **4**. These data can be obtained free of charge from the Cambridge Crystallographic Data Centre via www.ccdc.cam.ac.uk/data_request/cif. Supplementary data associated with this article can be found, in the online version, at doi:10.1016/j.ica.2008.12.012.

References

[1] S.J. Lipperd, J.M. Berg, Principles of Bioinorganic Chemistry, University Science Books, 1994.
[2] W. Kaim, B. Schwederski, Bioinorganic Chemistry: Inorganic Elements in the Chemistry of Life, Wiley, 1994.
[3] A.L. Gavrilova, B. Bosnich, Chem. Rev. 104 (2004) 349.
[4] A. Sigel, H. Sigel, R.K.O. Sigel (Eds.), Nickel and its Surprising Impact in Nature: Metal Ions in Life Sciences, Wiley, 2007.
[5] J. Weston, Chem. Rev. 105 (2004) 2151.
[6] F. Zippel, F. Ahlers, R. Werner, W. Haase, H.-F. Nolting, B. Krebs, Inorg. Chem. 35 (1996) 3409.
[7] O. Iranzo, A.Y. Kovalevsky, J.R. Morrow, J.P. Richard, J. Am. Chem. Soc. 125 (2003) 1988.
[8] K. Yamaguchi, S. Koshino, F. Akagi, M. Suzuki, A. Uehara, S. Suzuki, J. Am. Chem. Soc. 119 (1997) 5752.
[9] K. Yamaguchi, F. Akagi, S. Fujinami, M. Suzuki, M. Shionoya, S. Suzuki, Chem. Commun. (2001) 375.
[10] C. Fernandes, A. Neves, A.J. Bortoluzzi, A.S. Mangrich, E. Rentschler, B. Szpoganicz, E. Schwingel, Inorg. Chim. Acta 320 (2001) 12.
[11] P. Gamez, J. von Harras, O. Roubeau, W.L. Driessen, J. Reedijk, Inor. Chim. Acta 324 (2001) 27.
[12] T. Gajda, A. Jancsó, S. Mikkola, H. Lönnberg, H. Sirges, J. Chem. Soc., Dalton Trans. (2002) 1757.
[13] T. Gajda, R. Krämer, A. Jancsó, Eur. J. Inorg. Chem. (2000) 1635.
[14] N.S. Gonçalves, L.M. Rossi, L.K. Noda, P.S. Santos, A.J. Bortoluzzi, A. Neves, I. Vencato, Inorg. Chim. Acta 329 (2002) 141.
[15] C. Palopoli, M. González-Sierra, G. Robles, F. Dahan, J.-P. Tuchagues, S. Signorella, J. Chem. Soc., Dalton Trans. (2002) 3813.
[16] B. Krebs, K. Schepers, B. Bremer, G. Henkel, E. Althaus, W. Müller-Warmuth, K. Griesar, W. Haase, Inorg. Chem. 33 (1994) 1907.
[17] J.H. Satcher Jr., M.W. Droege, M.M. Olmstead, A.L. Balch, Inorg. Chem. 40 (2001) 1454.
[18] K. Mochizuki, K. Kashima, T. Weyhermüller, Inorg. Chem. Commun. 9 (2006) 891.
[19] K. Mochizuki, Y. Numata, Inorg. Chem. Commun. 7 (2004) 806.
[20] K. Mochizuki, A. Hasegawa, T. Weyhermüller, Inorg. Chim. Acta 357 (2004) 3245. and cited therein.
[21] K. Mochizuki, M. Shibazaki, T. Shiraishi, The 51st Symposium on Coordination Chemistry of Japan, (1P-B04), Matsue, 2001, p. 166 (abstract).
[22] A. Altomare, G. Cascarno, C. Giacovazzo, A. Gualiardi, J. Appl. Crystallogr. 27 (1994) 435.
[23] G.M. Sheldrick, University of Göttingen, Germany, 1997.
[24] A.C.T. North, D.C. Phillips, F.S. Mathews, Acta Crystallogr. A24 (1968) 351.
[25] L.J. Farrugia, J. Appl. Cryst. 30 (1997) 565.
[26] A.W. Addison, T.N. Rao, J. Chem. Soc., Dalton Trans. (1996) 1349.
[27] J. Hermann, A. Erxleben, Inorg. Chim. Acta 304 (2000) 125.
[28] A. Demsar, J. Kosmrlj, S. Petricek, J. Am. Chem. Soc. 124 (2002) 3951.
[29] E. Asato, H. Furutachi, T. Kawahashi, M. Mikuriya, J. Chem. Soc., Dalton Trans. (1995) 3897.
[30] M.M. Ibrahim, Inorg. Chem. Commun. 9 (2006) 1215.
[31] K. Weis, M. Rombach, M. Ruf, H. Vahrenkamp, Eur. J. Inorg. Chem. (1998) 263.
[32] J.A.M. Calvo, H. Vahrenkamp, Inorg. Chim. Acta 358 (2005) 4019.
[33] F. Gross, H. Vahrenkamp, Inorg. Chem. 44 (2005) 3321.
[34] M. Yamami, H. Furutachi, T. Yokoyama, H. Ōkawa, Inorg. Chem. 37 (1998) 6832.
[35] D. Kong, A.E. Martell, J. Reibenspies, Inorg. Chim. Acta 333 (2002) 7.
[36] M.M. Ibrahim, N. Shimomura, K. Ichikawa, M. Shiro, Inorg. Chim. Acta 313 (2001) 125.